Two-dimensional materials research

Guangyu Zhang*, Shixuan Du,
Kehui Wu, and Hong-Jun Gao

The National Research Center for Condensed Matter Physics and the Institute of Physics (IOP) of the Chinese Academy of Sciences have devoted much effort to many emerging frontiers in the field of condensed matter physics. In 2001, the Nanoscale Physics and Devices Laboratory was established at IOP, with a focus on nanoscale science and technology research. In recent years, the discovery of graphene, an atomically thin material possessing exotic physical properties and having wide-ranging potential applications, has boosted a new research field—the study of two-dimensional (2D) materials. This field has introduced many new concepts into conventional materials science, condensed matter physics, and electronic engineering.

Several research groups at IOP focus on 2D materials research, in order to design and create new materials with unexpected properties and tailoring, and to characterize the structures of 2D materials for elaborate band-structure modulation and functional device applications. The main research activities are described below.

Tailoring graphene by substrates and nanostructures

Graphene growth is usually assisted by a catalytic process. Fabrication of large-scale, high-quality graphene (G) is one of the main challenges in the field of graphene research. Hong-Jun Gao's group has successfully grown defect-free, single-crystalline graphene at the centimeter scale on ruthenium [Ru(0001)] with a highly ordered moiré pattern (*1, 2*). The pattern provides an ideal template for selective absorption of molecules, monodispersed metal atoms, or clusters (*3–10*). The periodic bumps behave like quantum dots with tunable thermoelectric properties. For practical application in nanoelectronic devices, Gao's group developed a technique to intercalate silicon and other elements at the G/Ru interface (Figure 1) (*11–13*) in order to decouple the interaction between graphene and metal crystals.

Since most of graphene-based electronic devices are fabricated on insulating substrates, scaled-up growth of high-quality graphene on insulating surfaces is of technological importance. To this end, Guangyu Zhang's group developed a catalyst-free, plasma-enhanced chemical vapor deposition (PECVD) technique to grow graphene on various insulating substrates at relatively

Institute of Physics, Chinese Academy of Sciences, Beijing, China
*Corresponding author: gyzhang@iphy.ac.cn

low growth temperatures (*14*). They also realized the epitaxial growth of nontwisted graphene on hexagonal boron nitride (G/h-BN) (*15, 16*). The large moiré superlattice originating from the nontwisting overlapping of graphene and h-BN had strong modulation effects on the band structure (Figure 2). Transport measurements on such superlattice samples revealed that superlattice Dirac points and Landau levels originated from the 2D superlattice. Owing to the clean interface, they could observe the fractal gaps of Hofstadter's butterfly, optical transitions between different Landau levels, and optical transitions between superlattice minibands (*17, 18*). Recently, Chen *et al.* characterized polaritons in G/h-BN and found that hyperbolic phonon polaritons in h-BN possess a high quality factor (Q ~ 33), ultraslow group velocity [~$2\times10^{-4}c$ (where *c* is the speed of light in a vacuum)], and a controll-able dispersion relation. They also identified a new hybridized polariton mode in G/h-BN with a long lifetime of ~1.6 ps (*19, 20*).

Zhang's group developed an anisotropic etching-based "top-down" fabrication technique for graphene nanostructures (Figure 2B) (*21, 22*). The as-fabricated graphene nanostructures have zigzag edge terminations and well-defined line widths (with sub-10 nm resolution capability), benefiting from the anisotropic etching effect in graphene's basal plane. Such zigzag graphene nanostructures are ideal experimental objects for investigating the quantum confinement effect, edge-state related transport, and valleytronics in graphene.

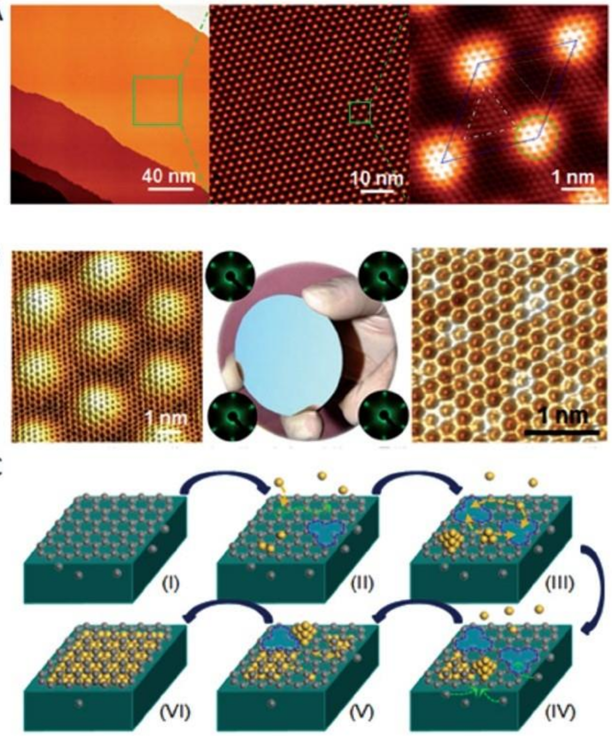

FIGURE 1. Epitaxial graphene and Si intercalation. (**A**) Scanning tunneling microscope (STM) images of graphene/ruthenium (G/Ru). (**B**) STM images of G/Ru (left) and after silicon (Si) intercalation (right). Low-energy electron diffraction (LEED) pattern (middle) of the entire sample indicates high-quality graphene over the entire surface. (**C**) Schematic of Si intercalation process.

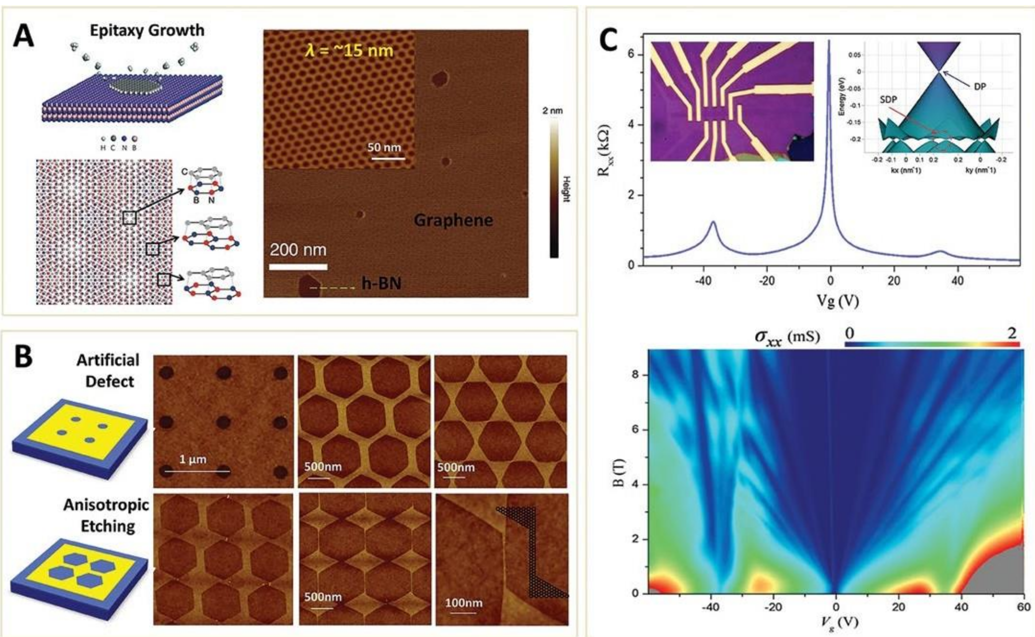

FIGURE 2. Engineering of graphene superlattice and nanostructures. (**A**) Graphene (G) epitaxy on hexagonal boron nitride (h-BN): A 2D superlattice structure. (**B**) Fabrication of graphene nanostructure by anisotropic etching. (**C**) Transport measurements on G/h-BN superlattice.

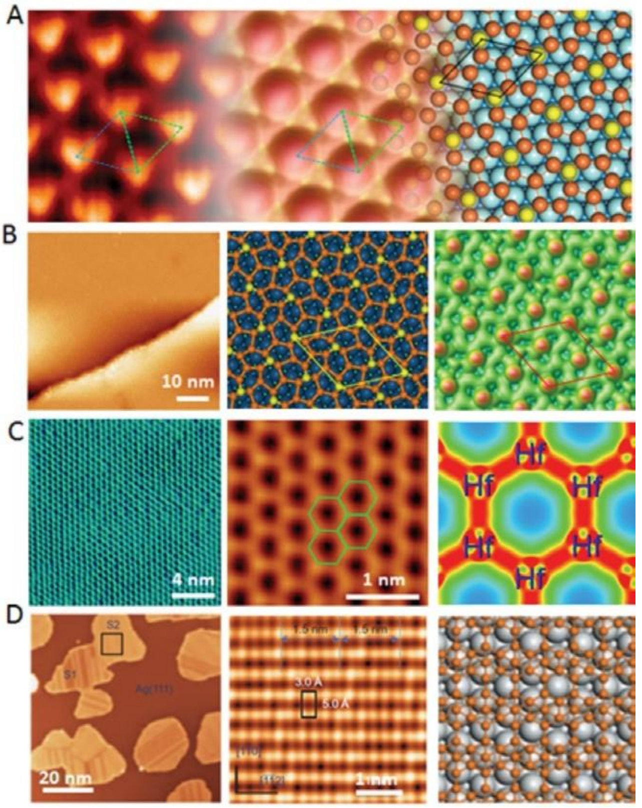

FIGURE 3. Epitaxial Xene on metal substrate. (A) Scanning tunneling microscope (STM) images and configuration of silicene/iridium [Ir(111)]. (B) STM image, configuration, and STM simulation of germanene/platinum [Pt(111)]. (C) STM images and charge density of hafnene/Ir(111). (**D**) STM images and configuration of borophene/silver [Ag(111)].

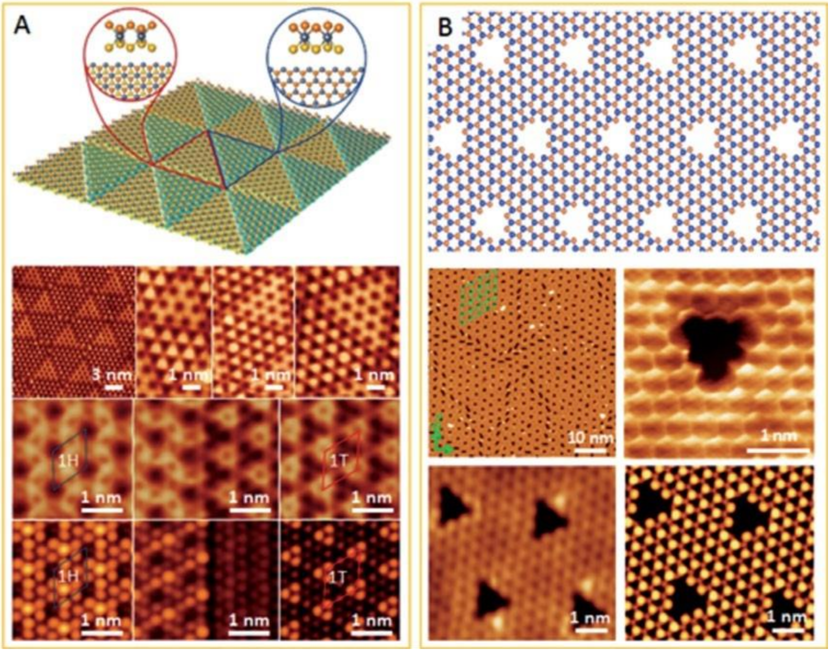

FIGURE 4. Intrinsically patterned 2D materials. (**A**) Patterned platinum diselenide (PtSe2) monolayer: schematic, scanning tunneling microscope (STM) images, and STM simulations. (**B**) Patterned copper selenide (CuSe) monolayer: schematic, STM images, and STM simulation.

Single-element 2D materials beyond graphene

Novel 2D materials can be epitaxially grown on single-crystal surfaces. Gao's and Wu's groups conducted pioneering studies on silicene with a honeycomb lattice epitaxy in ultrahigh vacuum (UHV) on iridium [Ir(111)] and silver [Ag(111)], respectively (Figure 3) (*23, 24*). Gao's group found that the growth of silicene on Ru(0001) evolves from a herringbone structure toward a buckled honeycomb lattice. Wu's group found that such a buckled honeycomb lattice could host the Dirac cone structure in the energy bands, and that hydrogenation of silicene is an effective way to protect it from oxidation (*25, 26*).

Gao's group is the first to create germanene and hafnene (Figure 3B, 3C) (*27–29*). Further experiments provide evidence of the Dirac signature in bilayer germanene on copper [Cu(111)]. The honeycomb lattice of hafnene is metallic with a spin-polarized *d*-dominated state near the Fermi level. Wu's group reported the realization of 2D boron sheets by molecular beam epitaxy (MBE) (Figure 3D). Two types of boron sheets comprising a triangular boron lattice with different arrangements of hexagonal holes have been identified and are quite stable against oxidization. Dirac cones in the energy band of 2D boron sheets were also revealed (*30, 31*).

Binary 2D materials beyond graphene

Binary 2D materials have enhanced properties and diverse materials options. Gao's group developed a direct selenization method to grow selenide monolayers in a UHV chamber by standard molecular beam epitaxy (MBE) (*32*). With this simple process, they successfully synthesized platinum diselenide ($PtSe_2$), hafnium tritelluride ($HfTe_3$), hafnium pentatelluride ($HfTe_5$), and copper selenide (CuSe) monolayers. Direct tellurization of Hf(0001) results in the spontaneous fabrication of a

$HfTe_3$-$HfTe_5$-Hf lateral heterostructure (*33*), which offers new routes for the construction of related functional heterostructures. Moreover, Gao's group found that $PtSe_2$ and CuSe monolayers are intrinsically patterned (Figure 4) (*34*), and are thus ideal templates for selective adsorptions of either molecules or magnetic metal– containing clusters. Spin-layer locking by local Rashba effect in the as-synthesized 1T-$PtSe_2$ was observed, indicating that 1T-$PtSe_2$ is a promising photocatalyst and valleytronic material.

Besides the surface reaction process, the standard chemical vapor deposition (CVD) process provides another option to grow binary 2D materials directly on insulating substrates. Zhang's group developed an oxygen-assisted CVD method for the growth of high- quality monolayer molybdenum disulfide (MoS_2) (*35, 36*). Using this method, they grew wafer-scale, highly oriented, and continuous monolayer MoS_2, representing a significant step toward the realization of wafer-scale monolayer MoS_2 devices for potential electronic and optoelectronic applications (*36*). Recently, they found that an argon (Ar)-plasma treatment could locally induce 2H-1T phase transition in monolayer MoS_2 (*37*).

Device applications based on 2D materials

Exploration of 2D materials for certain novel applications has been a driving force in this field. Zhang's group explored various 2D material-based nanodevices for electronic applications, such as graphene nanoelectromechanical system (NEMS) switch devices, ultrasensitive graphene strain sensors and electronic skin, graphene-based charge-trapping memories, and graphene nanogap multilevel memristor devices (*38–46*). They also demonstrated highly sensitive humidity sensors based on monolayer MoS_2 films with clean surfaces. Moreover, they explored graphene-contacted ultrashort channel monolayer MoS_2 field-effect transistors with channel lengths scaled down to ~4 nm, exhibiting excellent immunity to short-channel effects.

In summary, 2D materials research at IOP has rapidly developed over the past decade. A series of studies have been devoted to 2D materials with a focus on developing state-of-the-art epitaxial growth techniques by probing and manipulating their atomic, electronic, optical, and magnetic structures using advanced characterization techniques, and exploring their potential applications in electronics, optoelectronics, and spintronics.

References

1. Y. Pan, D.-X. Shi, H.-J. Gao, *Chin. Phys.* **16**, 3151 (2007).
2. Y. Pan *et al., Adv. Mater.* **21**, 2777–2780 (2009).
3. J. Mao *et al.*, *J. Am. Chem. Soc.* **131**, 14136–14137 (2009).
4. H. T. Zhou *et al.*, *Appl. Phys. Lett.* **99**, 153101 (2011).
5. H. G. Zhang *et al.*, *Phys. Rev. B* **84**, 245436 (2011).
6. G. Li *et al.*, *Appl. Phys. Lett*. **100**, 013304 (2012).
7. H. G. Zhang *et al.*, *J. Phys. Cond. Matter* **22**, 302001 (2010).
8. J. D. Ren *et al.*, *Phys. Rev. Lett*. **119**, 176806 (2017).
9. Y. Pan, M. Gao, L. Huang, F. Liu, H.-J. Gao, *Appl. Phys. Lett.* **95**, 093106 (2009).
10. J. D. Ren *et al.*, *Nano Lett.* **14**, 4011–4015 (2014).
11. G. Li *et al.*, *J. Am. Chem. Soc.* **137**, 7099–7103 (2015).
12. L. Huang *et al.*, *Appl. Phys. Lett.* **99**, 163107 (2011).
13. J. H. Mao *et al.*, *Appl. Phys. Lett.* **100**, 093101 (2012).
14. L. C. Zhang *et al.*, *Nano Res.* **4**, 315–321 (2011).
15. W. Yang *et al.*, *Nat. Mater.* **12**, 792–797 (2013).
16. W. Yang *et al.*, *Nano Lett.* **16**, 2387–2392 (2016).
17. Z. W. Shi *et al.*, *Nat. Phys.* **10**, 743–747 (2014).
18. Z. G. Chen *et al.*, *Nat. Commun.* **5**, 4461 (2014).
19. J. H. Duan *et al.*, *Adv. Mater.* **29**, 1702494 (2017).
20. X. X. Yang *et al.*, *Adv. Mater.* **28**, 2931–2938 (2016).
21. R. Yang *et al.*, *Adv. Mater.* **22**, 4014–4019 (2010).
22. Z. Shi *et al.*, *Adv. Mater.* **23**, 3061–3065 (2011).
23. B. J. Feng *et al.*, *Nano Lett.* **12**, 3507–3511 (2012).
24. L. Meng *et al.*, *Nano Lett.* **13**, 685–690 (2013).
25. L. Chen *et al.*, *Phys. Rev. Lett.* **109**, 056804 (2012).
26. J. L. Qiu *et al.*, *Phys. Rev. Lett.* **114**, 126101 (2015).
27. L. F. Li *et al.*, *Adv. Mater.* **26**, 4820–4824 (2014).
28. Z. H. Qin *et al.*, *Adv. Mater.* **29**, 1606046 (2017).
29. L. F. Li *et al.*, *Nano Lett.* **13**, 4671–4674 (2013).
30. B. J. Feng *et al.*, *Nat. Chem.* **8**, 563–568 (2016).
31. B. Feng *et al.*, *Phys. Rev. Lett.* **118**, 096401 (2017).
32. Y. Wang *et al.*, *Nano Lett.* **15**, 4013–4018 (2015).
33. Y. Q. Wang *et al., Adv. Mater.* **28**, 5013–5017 (2016).
34. X. Lin *et al.*, *Nat. Mater.* **16**, 717–721 (2017).
35. W. Chen *et al.*, *J. Am. Chem. Soc.* **137**, 15632–15635 (2015).
36. H. Yu *et al.*, *ACS Nano* **11**, 12001–12007 (2017).
37. J. Zhu *et al.*, *J. Am. Chem. Soc.* **139**, 10216–10219 (2017).
38. Z. Shi *et al.*, *Nano Res.* **5**, 82–87 (2012).
39. Y. Wang *et al.*, *ACS Nano* **5**, 3645–3650 (2011).
40. J. Zhao *et al.*, *Appl. Phys. Lett.* **101**, 063112 (2012).
41. J. Zhao *et al.*, *ACS Nano* **9**, 1622–1629 (2015).
42. R. Yang *et al.*, *Sci. Rep.* **3**, 2126 (2013).
43. C. He *et al., ACS Nano* **6**, 4214–4221 (2012).
44. C. He *et al.*, *Adv. Mater.* **25**, 5593–5598 (2013).
45. J. Zhao *et al.*, *Adv. Mater.* **29**, 1702076 (2017).
46. L. Xie *et al.*, *Adv. Mater.* **29**, 1702522 (2017)